Anuário do Instituto de Geociências
Universidade Federal do Rio de Janeiro
https://revistas.ufrj.br/index.php/aigeo/

ISSN 0101-9759
e-ISSN 1982-3908

New Methodology for Precise UAV Surveys with a Single Ground Control Point

Nova Metodologia para Levantamentos de Precisão com VANT com um Único Ponto de Controle em Solo

Marciano Carneiro[1], Rodrigo de Lemos Peroni[1], Alexandre Felipe Bruch[2], Angélica Cirolini[2] & Adriane Brill Thum[3]

[1]Universidade Federal do Rio Grande do Sul, Centro de Engenharia, Porto Alegre, RS, Brasil
[2]Universidade Federal de Pelotas, Centro de Engenharias, Pelotas, RS, Brasil
[3]Universidade do Vale do Rio dos Sinos, Centro de Engenharia, São Leopoldo, RS, Brasil

E-mails: marciano.carneiro@hotmail.com; 00015547@ufrgs.br; afbruch@gmail.com; acirolini@gmail.com; adrianebt@unisinos.br
Corresponding author: Marciano Carneiro; marciano.carneiro@hotmail.com

Abstract

The advances in aerial mapping using unmanned aerial vehicles (UAVs) are increasingly allowing for the surveying of areas that are difficult or unsafe to access. Considering that the cameras boarded on UAVs are non-photogrammetric sensors, positional accuracy and precision are paramount to ensuring that the final product is geometrically consistent and that its coordinates are precise enough within an acceptable range (which depends on the purpose of each application). With this in mind, this work evaluates the positional accuracy of aerial surveys with UAVs supported by the post-processed kinematic (PPK) technique for the generation of cartographic products in compliance with the Brazilian cartographic accuracy standard PEC-PCD. Furthermore, this study proposes a methodology for inserting virtual control points using coordinates adjusted and inserted into the main point of selected images, using the package of solutions for GNSS RTKLIB processing, to forgo Ground Control Points (GCPs) without loss of quality of the cartographic product. This research used a UAV from DJI (model Mavic 2 Pro), equipped with a dual frequency GNSS receiver, where positional records were synchronized with the camera's shooting times. To validate the technique, 20 checkpoints with known coordinates were selected, and these points were used in statistical tests to assess the accuracy and precision of the survey. The orthomosaic and the digital elevation model were used as the reference for positional coordinates to be compared against the PEC-PCD standards. The results show that the discrepancy is, on average, 0.126 m for planimetric coordinates and 0.066 m for altimetry. No outliers were found, suggesting a Gaussian sampling distribution. The application of Student's t-test indicated the existence of a small bias, suggesting the displacement of coordinates along the three axes. The chi-square test showed results below the tabulated limits, attesting to the high precision of the survey. Finally, the root mean squared error (RMSE) was lower than the standard error limit for PEC-PCD class A planialtimetric cartographic products on a 1:1,000 scale. The viability of this technique is thus confirmed.

Keywords: Cartographic accuracy standard; PPK; Mapping

Resumo

O avanço no mapeamento aéreo tem possibilitado cada vez mais o levantamento cartográfico de áreas de difícil acesso ou de risco. Nesse sentido, este trabalho avalia a acurácia posicional de aerolevantamentos com Aeronave Remotamente Pilotada (ARP), apoiado pela técnica *Post Processed Kinematic* (PPK), para a geração de produtos cartográficos enquadrados no Padrão de Exatidão Cartográfica (PEC) brasileiro. Esta pesquisa utilizou o VANT Mavic 2 Pro, sendo embarcado um receptor GNSS de dupla frequência, com registros posicionais sincronizados com o disparo da câmera. O plano de voo foi criado no programa *DroneDeploy.* Esse estudo propõe uma metodologia de inserção de pontos de controle virtuais com coordenadas ajustadas e inseridas no Ponto Principal das imagens, através do pacote de soluções para processamento GNSS RTKLIB para acelerar os levantamentos sem perda da qualidade e precisão do produto cartográfico. Foram materializados 20 pontos de checagem com coordenadas conhecidas, sendo estes utilizados nos testes estatísticos para avaliar a acurácia e precisão do levantamento. O ortomosaico e o Modelo Digital de Superfície serviram de origem para as coordenadas posicionais testadas e comparadas com a PEC-PCD. Os resultados demonstram que a média da discrepância planimétrica é de 0,126m e 0,066m na altimetria. Não foram encontrados *outliers*, considerando-se uma amostragem gaussiana. A aplicação do teste *t* de Student, indicou a existência de tendência nos três eixos calculados. O teste qui-quadrado apresentou resultados abaixo dos limites tabelados, atestando alta precisão ao levantamento. Por fim, o Erro Quadrático Médio também foi inferior ao Erro Padrão esperado para a geração de produtos cartográficos planialtimétricos classe A da PEC-PCD, na escala 1:1.000, demonstrando assim a viabilidade desta técnica.

Palavras-chave: Padrão de precisão cartográfica; PPK; Mapeamento

Received: 05 July 2021; Accepted: 23 August 2021

1 Introduction

Thanks to the continuous development of geotechnologies, mapping with high temporal and spatial resolution has become possible. Low-cost aerial surveys can be done using equipment known as unmanned aerial vehicles (UAVs), associated with the use of the Global Navigation Satellite System (GNSS) (Munaretto 2017). The use of UAVs in technical and scientific works has increased rapidly over the last decade in several areas, including mining, environmental sciences, and earth sciences These devices allow more precise surveys, more accurate measurements, and more frequent inspections than had previously been possible (Munaretto 2017; Ribeiro 2011).

To perform image rectification, some field procedures are necessary, especially collection of ground coordinates for the visually identifiable natural and artificial targets in the photos. Normally, the spatial distribution of these targets must be sufficient for adequate coverage of the target area, as well as to allow for easy and precise identification of the images using aerophotogrammetric software (Bolkas 2019). These tasks are not always simple, and can slow down the process and increase costs.

An alternative to the use of physical targets is to obtain the coordinates of the sensor at the exact moment when each image/photo is obtained. Some UAV manufacturers produce devices that guarantee synchronization of the photos taken by the camera with the aircraft's position record, using relative methods combining real-time positions with telemetry methods such as real time kinematic positioning (RTK) or even post-processing using post-processed kinematic (PPK). The two methods provide millimetric positional accuracy, both horizontal and vertical (Lose, Chiabrando & Tonolo 2020). This work aims to contribute to the cartographic knowledge based on mapping with UAVs. We propose a way to speed up the process and offer solutions for areas that are difficult to access to retrieve ground control points.

2 Cartographic Accuracy Standard (PEC-PCD)

An important milestone in Brazilian cartography was the regulation of Decree-Law No. 89,817 from June 20th, 1984 (BRASIL 1984), which standardizes the criteria for the classification of national cartographic products according to their accuracy. It is called the Cartographic Accuracy Standard (PEC-PCD). When real coordinates are taken with high-precision GNSS equipment in the field, the standard specifies that 90% of the validation points should not present an error greater than the given limits for each class with respect to the coordinates in the cartographic product. This threshold is important because it guides statistical tests (Santos 2016; Bruch et al. 2019). In conceptual terms, this decree is also important because it uses terms such as Standard Deviation (SD), Standard Error (EP), and Mean Square Error (MSE) (all used interchangeably), in addition to the terms "accuracy" and "positional accuracy" (BRASIL 1984). Therefore, in agreement with the National Cartography Commission (CONCAR), the digital product can be accepted as a reference product for the National Cartographic System (SCN), and, consequently, for the National Spatial Data Infrastructure (INDE). For products printed on paper, 90% or 1.64 *RMS of the errors in the points collected in the cartographic/topographic product (orthography or orthomatics) must present values equal to or less than the tolerance limits provided by the PEC-PDC (Table 1).

Table 1 PEC-PCD for Digital Model of Surface (MDS), Digital Model of Ground (MDT), and Digital Model of Elevation MDE, and quoted points.

PEC	PEC-PCD	1:1,000 (Eqd = 1 m)		1:2,000 (Eqd = 1 m)		1:5,000 (Eqd = 2 m)		1:10,000 (Eqd = 5 m)		1:25,000 (Eqd = 10 m)		1:50,000 (Eqd =20 m)		1:100,000 (Eqd = 50m)		1:250,000 (Eqd = 100m)	
		PEC (m)	EP (m)	PEC (m)	EP (m)	PEC (m)	EP (m)	PEC (m)	EP (m)	PEC (m)	EP (m)	PEC (m)	EP (m)	PEC (m)	EP (m)	PEC (m)	EP (m)
–	A	0.27	0.17	0.27	0.17	0.54	0.34	1.35	0.84	2.70	1.67	5.50	3.33	13.70	8.33	27.00	16.67
A	B	0.50	0.33	0.50	0.33	1.00	0.66	2.50	1.67	5.00	3.33	10.00	6.66	25.00	16.66	50.00	33.33
B	C	0.60	0.40	0.60	0.40	1.20	0.80	3.00	2.00	6.00	4.00	12.00	8.00	30.00	20.00	60.00	40.00
C	D	0.75	0.50	0.75	0.50	1.50	1.00	3.75	2.50	7.50	5.00	15.00	10.00	37.50	25.00	75.00	50.00

Source: CONCAR (2011).

3 Materials and Methods

The study area is an aggregate quarry mine, which produces classified gravel for construction. It presented a range of elevations, slopes, and ramps, and lacked vegetation, guaranteeing a full view of the ground. This allows geometries and topographic conditions to be analyzed.

The quarry is in the southern region of Brazil, in the municipality of Pelotas/RS (Figure 1). It has an area of about 10 hectares, and the center has the east/north coordinates of 362,775 m and 6,499,125 m of the zone 22S/UTM. The orthomosaic generated in MetaShape has a ground sampling distance (GSD) of 2.84 cm. The altimetric amplitude found in the digital surface model (MDS) was 49.333 meters, with a minimum orthometric altitude of 111.40 m and a maximum of 160.74 m.

This section presents the materials and methods used in the process of assessing the accuracy of aerial surveys with UAVs, aided by spatial positioning using the PPK technique, as shown in Figure 2. We describe the equipment and procedures used both in the field and in the office.

3.1 Unmanned Aerial Vehicle (UAV)

In the development of this research, a multirotor UAV was used, manufactured by the company DJI, model Mavic 2 Pro. The descriptions of the equipment characteristics and the flight plan are presented in Table 2. The flight took place at 11:30 AM. The schedule was based on the daylight hours with the lowest solar inclination so as to minimize shadows on the images taken.

3.2 Determination of the Base Control Point and Checkpoint Coordinates

In this work, only one control point was used, called the base control point, to increase the accuracy of the survey, mainly for the altimetric coordinates. According to Monico (2008), the Z axis is the one with the greatest embedded error, especially in kinematic surveys with GNSS receivers. According to Lose, Chiabrando & Tonolo (2020), a single control point is sufficient to correct vertical displacement in aerial surveys aided by the PPK technique.

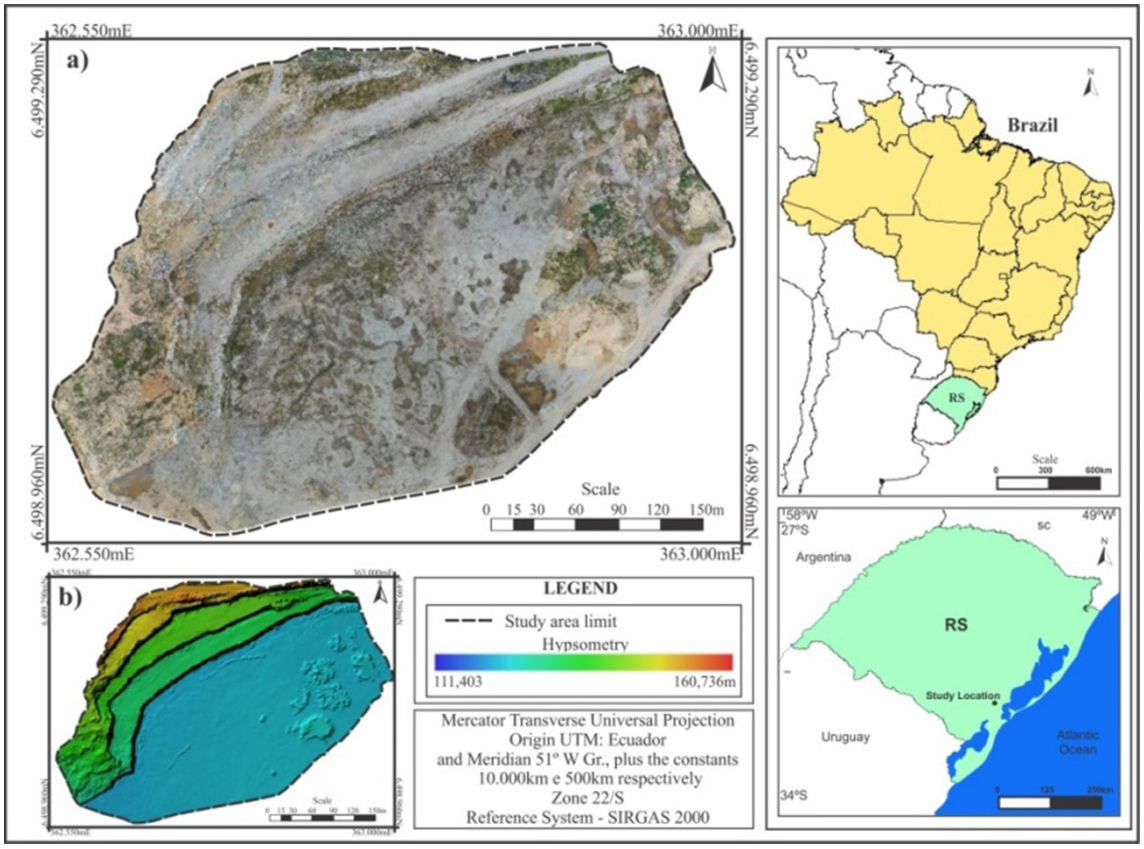

Figure 1 A map of the study area.

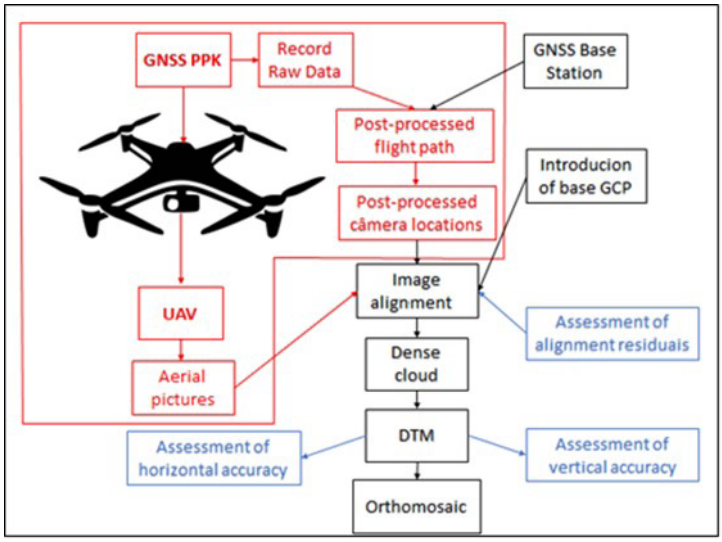

Figure 2 Methodological flowchart.

Table 2. Characteristics of the UAV and the flight plan used in the aerial survey.

Equipment features	Flight plan characteristics
Flight order weight: 907 g	Flight altitude: 100 m
Flight time: 31 minutes	Lateral overlap of the bands: 60%
Maximum transmitter radio range: 10 km	Front overlay of photos: 70%
Battery: 3850 mAh LiPo4s	Flight azimuth: 8th
Camera: 20-megapixel CMOS sensor	Maximum speed: 10 m/s
Maximum dimension of each photo: 5472 x 3648 pixels	Aim of the camera: nadir
Shutter speed: 8-1 / 8000 s	Spatial resolution: 2.3 cm / pixel
Camera field of view: 77º	Flight time: 11 minutes and 24 seconds
Spatial Positioning: GPS + GLONASS	Number of images: 187

Source: DJI (2021).

The geodetic coordinates of 20 checkpoints were also determined and used to calculate the positional accuracy of the orthomosaic and MDS to validate the methodology. In this process, a pair of GNSS receivers (model Emlid Reach RS2) was used to receive corrections in real time (RTK).

To represent and mark each of the checkpoints and the base control point, several canvas targets were made in two contrasting colors, with dimensions of 40 × 40 cm, as shown in Figure 3.

The geodesic reference system used was the SIRGAS 2000, and the projection was the Universal Transverse Mercator (UTM) Zone 22S.

3.3 Post-Processed Kinematics (PPK)

The post-processed kinematic technique (PPK) has been widely used in aerial surveys. In this technique, a GNSS receiver stores the observables at a known point, serving as a reference station. They are later used to adjust the points registered by the receiver embedded in the UAV. Unlike the RTK technique, this does not require a telemetry connection in real time (Bolkas 2019; Taddia, Stecchi & Pellegrinelli 2020; Tomastík et al. 2019; Zhang et al. 2019).

For the PPK technique, the same GNSS receiver (Emlid Reach RS2) was used as the base station. An additional Emlid GNSS receiver (model Reach M2) was carried on the UAV. To connect the structure of the receiver to the antenna, a supporting case was made with a 3D printer according to the design presented in Figure 4. To record the moment when the UAV camera's shutter was triggered, a photosensitive sensor was adapted in conjunction with the light, and this was used to record the position of the equipment at the time each image was taken.

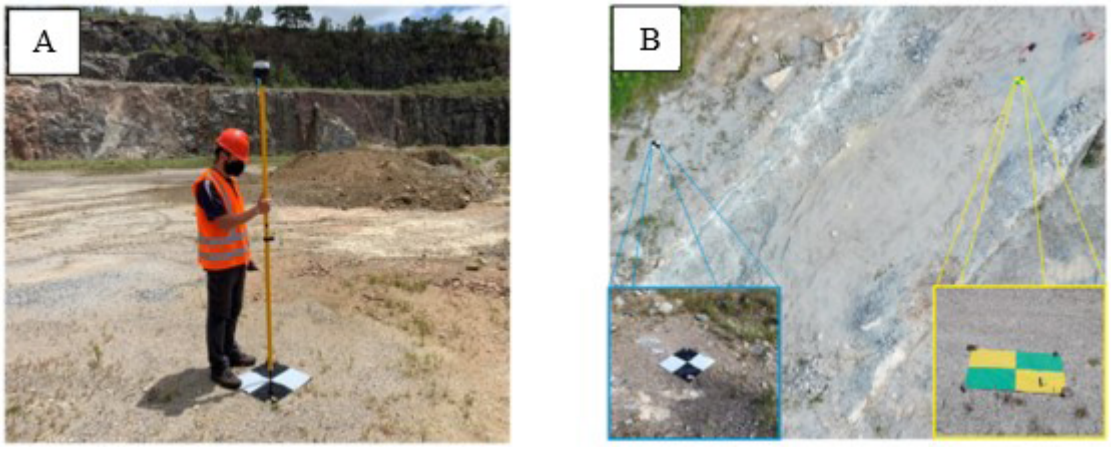

Figure 3 A. Determination of geodetic coordinates; B. materialization of the checkpoints and control point.

Figure 4 The mounting case for the receiver and the antenna.

The GNSS base was assembled and configured to record raw data in the UBX format. The flight plan was then executed, and the GNSS Reach M2 (L1/L2) board stored the positional coordinates when the UAV camera took each photo, resulting in a log file for further processing.

After the execution of the flight plan, the UAV receiver file was processed by the relative positioning processing technique using the coordinates from the base (taken from the Positioning by Precise Point (PPP) processing). To execute this step, double differences (DDs) were used as fundamental observables. In this technique, two or more connected receivers simultaneously track at least two of the same satellites (Collischonn & Matsuoka 2016). The baseline positions (ΔX, ΔY and ΔZ) between two or more occupations are estimated. During this process, the components that are part of the baseline are estimated, and, when added to the coordinates of the base point, generate the coordinates of the desired station (Monico 2008).

3.4 Image Processing

To process the aerial images, the Agisoft MetaShape Pro® program was used. MetaShape recognizes the images captured by different UAVs and cameras. This enables the creation of orthomosaics combining individual images based on the radiometric similarities between pairs or sets of overlapping images using their positional coordinates (Taddia, Stecchi & Pellegrinelli 2020; Zhou et al. 2020).

The processing began with visually checking the quality of the images and verifying that the number of photos taken by the UAV camera was the same as the number of positions in the log file generated by the coupled GNSS receiver. The images were imported, and the native coordinates registered by the UAV's GNSS receiver were replaced with the stored post-processed coordinates taken by the Emlid Reach M2 receiver. This was done by importing an exchangeable image file format (EXIF) file, exported in post-processing in RTKPOST, containing the corrected coordinates of the main point (PP) of each image.

In the next step, the images were aligned (Figure 5). The program was used to determine the parameters of the camera, the PPs, and the eventual rotation of the photos.

To generate accurate products through UAV surveys, with precision on the centimeter scale, Bolkas (2019), Tomastik et al. (2019), Zhang et al. (2019), Zhou et al. (2019), Taddia, Stecchi & Pellegrinelli (2020), Yu et al. (2020), and Zhou et al. (2020) all recommend using at least one control point to calibrate cameras with a scanning

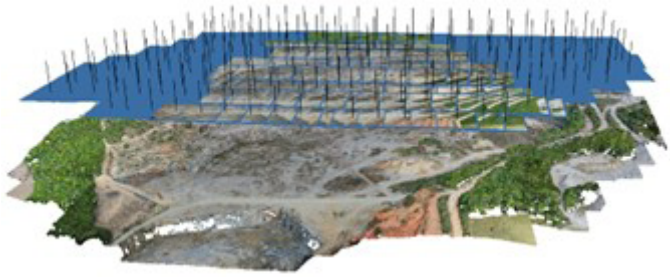

Figure 5 Alignment of the images.

sensor of the complementary metal oxide semiconductor (CMOS) type. Eight parameters are generally used: the focal length (f); the main points as X and Y coordinates (ppx, ppy); coefficients of the third order symmetric radial distortion polynomial (k1, k2. K3) described in Eq. (1); and the tangential distortion coefficients (P1, P2) expressed in Eq. (2). Two complementary parameters may also be used: the affinity and non-orthogonality parameters (b1, b2), defined according to Eq. (3).

$$\Delta r = k1r3 + k2r5 + k3r7 \quad (1)$$

$$\Delta x_d = P_1(r^2+2x^2) + 2P_2xy$$

$$\Delta y_d = 2P_1xy+P_2(r^2+2y^2) \quad (2)$$

$$r^2 = x^2+y^2=(x - PP_x)^2 + (y-PP_y)^2$$

$$\Delta x_a = b_1x+ b_2y \quad (3)$$

By inserting a control point, the parameters are estimated and adjusted for the construction of a dense point cloud. The control point used here was the UAV 1takeoff point, assumed to be the reference for the entire photogrammetric survey.

After the dense point cloud was generated, the MDS and the orthomosaic were built, allowing the coordinates (X and Y in the orthomosaic and Z in the MDS) to be extracted for the assessment and validation of the positional accuracy. In the generation of these products, MetaShape uses multiview technology, which can process arbitrary images with variable overlap, provided that the same points appear in different images (Bruch et al. 2019; Zhou et al. 2020).

3.5 Assessment of Positional Accuracy

According to the American National Standard for Spatial Data Accuracy (NSSDA) of 1998, at least 20 checkpoints are required for an adequately reliable statistical analysis. Authors such as Bolkas (2019), Tomastik et al. (2019), Zhang et al. (2019), Zhou et al. (2019), and Yu et al. (2020) use less than 20 checkpoints (12 or more), but they agree with the NSSDA standard in theory and emphasize that at least 20 checkpoints would be ideal. It is worth mentioning that good spatial distribution of the checkpoints is also important, across different mining benches and different elevations, covering the boundaries of the study area, as proposed by Santos et al. (2016a), Bruch et al. (2019), and Yu et al. (2020). Santos et al. (2016a) propose the use of the deterministic method of the nearest neighbor, where the R index is obtained by means of the observed average of the distance to the nearest neighbor, divided by the expected average for a random distribution of points. This process was implemented in the Georeferenced Information Processing System (SPRING) version 5.5.6.

Consequently, a comparison was made between the reference (R) coordinates, which were determined with the GNSS in the field, and the test (T) coordinates, which were extracted from the orthomatic and MDS, using Eq. (4) for the three coordinate axes (C). In this process, the planimetric discrepancy (Δ2d) was also calculated according to Eq. (5). The results were compared to the limits of accuracy and precision established by the PEC-PCD.

$$\Delta C = (C_T - C_R) \quad (4)$$

$$\Delta_{2d} = \sqrt{(X_T - X_R) + (Y_T - Y_R)}^2 \quad (5)$$

With the same data, the average statistic (Eq. 6) and the standard deviation (Eq. 7) were generated for the X, Y, and Z axes, where n is the total number of samples.

$$\overline{\Delta C} = \frac{1}{n}\sum_{i=1}^{n}\Delta C \quad (6)$$

$$S_{\Delta C} = \sqrt{\frac{1}{n-1}}\sum_{i=1}^{n}(\Delta C - \overline{\Delta C})^2 \quad (7)$$

Then the Student's t sample was calculated to check whether the result was in the range of acceptance or rejection of the null hypothesis (Elias et al. 2017). The t-test was applied considering a confidence interval (1 − α) equal to 90% (α = 0.10), and calculated according to Eq. 8 for the three coordinate axes.

$$t_c = \frac{\overline{\overline{\Delta C}}}{S_{\Delta C}}\sqrt{n} \quad (8)$$

Therefore, based on the number of checkpoints collected in the field, a limit t value (n − 1, α / 2) was found, which can be obtained from the tabulated values according to Eq. 9. If the value of Student's t-test is lower than the tabulated limit value for the variables X, Y, and Z analyzed, then it can be said that the product under evaluation presents the value of the mean of the positional discrepancies statistically equal to zero. This would mean that the product can be assumed not to show bias in its coordinates and to be free of systematic errors (Menezes et al. 2019).

$$\left|t_{calc}\right| < t_{n-1:\alpha/2} \quad (9)$$

For accuracy analysis, Silva (2015), Alves et al. (2015), Elias et al. (2017), and Bruch et al. (2019) recommend the chi-square test and the framework established in the Technical Specification for quality control of geospatial data (ET-CQDG) (DSG 2016). With a known expected standard error (σC) for a given axis of the coordinates (C), a hypothesis test is applied. The standard deviation of the height discrepancies is compared with the expected EP for the PEC-PCD class that needs to be complied with; H0: $S\Delta C^2 = \sigma C^2$, against H1: $S\Delta C^2 > \sigma C^2$ (Silva et al. 2016; Bruch et al. 2019). The xC2 value of the chi-square test calculated according to Eq. 10 must be lower than the table chi-square test x_ (n − 1, α)^2 shown in Eq. 11, making it possible to determine the scale of representation at which the orthomosaic and the MDS fall within classes A, B, C, and D. The sample size is represented by n; s is the standard deviation of the discrepancies; and σ is the expected EP for a given PEC-PCD class.

$$x_C^2 \leq X_{n-1,a}^2 \quad (10)$$

$$x_{c^2} = (n-1\frac{s_{\Delta C}^2}{\sigma_C^2} \quad (11)$$

4 Results and Discussion

As described in section 3.5, a statistical test of the nearest neighbor was applied to the 20 checkpoints, and the results show that there is a scattered pattern in the three orders analyzed, with an R index equal to 1.5508 in the first order, 1.2486 in the second order, and 1.1748 in the third order. According to Merchant (1982), Montgomery and Runger (2016), and Santos et al. (2016a), the presence of scattered or random patterns in at least three orders validates the checkpoints as spatial data of statistical reference. The dispersion according to the area varied from 0.000157 to 0.000215 points per m2, as shown in Figure 6.

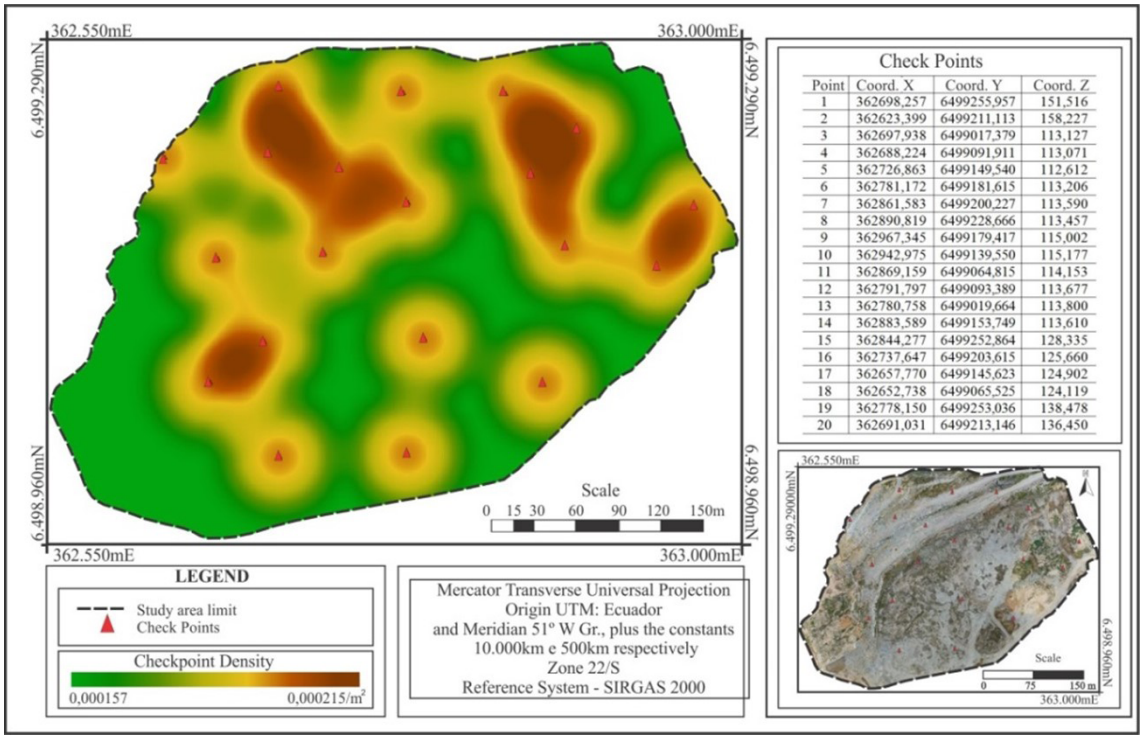

Figure 6 Distribution and density of the checkpoints.

As this work seeks to create a UAV aerial survey methodology based on the PPK technique, the positions of the 187 images were adjusted in RTKPOST for post-processing, and the positional records were validated for import into MetaShape. First, image alignment was performed and a sparse cloud of points was generated. The control point was imported and the camera parameters were estimated. The calibrated focal length was set as 4.473 mm; the coordinates of ppx and ppy were 2.425 and 1.823, respectively. The third order symmetric radial distortion coefficients in were k1 0.012, k2 −0.065 and k3 0.107. The tangential distortion coefficients P1 and P2 had values of −0.001 for both. Finally, the affinity and non-orthogonality parameters (b1 and b2) had values of 0.501 and −0.143, respectively.

Alves et al. (2015), Fonseca Neto et al. (2017), and Oliveira and Brito (2019) discuss the feasibility of using aerial surveys, carried out with UAVs and supported by ground control points, to generate an accurate planimetric cartographic product that could be accepted as class A PEC-PCD at a 1:1,000 scale. This was suggested in the work of Santos et al. (2016a) and Bruch et al. (2019) for the elaboration of altimetric cartographic products in the same class and scale.

The averages of the discrepancies were −0.081, 0.093, and 0.126 m on the E, N, and Z axes, respectively, with an average planimetric positional discrepancy (ΔP) of 0.126 m (Figure 7). According the PEC-PCD, for an accurate product, 90% of the points must show discrepancies below 0.28 cm in the planimetry and below 0.27 in the altimetry; in this research, all the checkpoints showed discrepancies smaller than that (Table 3). The standard deviation followed the results of the mean, with 0.059, 0.050, and 0.033 m on the E, N, and Z axes, with a planimetric standard deviation of 0.053 m.

Similar results were found by Alves et al. (2015), Silva et al. (2016), Fonseca Neto et al. (2017), Fonseca Neto (2018), and Bruch et al. (2019); all these works used control points. In terms of PPK positioning, similar results have been described by Zhang et al. (2019), Yu et al. (2020), Lose, Chiabrando, & Tonolo (2020), and Kurkov and Kiseleva (2020), using the UAV DJI Phantom 4 ADV/PRO.

For the detection of eventual outliers, the boxplots for the planimetric and altimetric discrepancies (represented in Figure 8) were elaborated. The absence of outliers was verified, lending reliability to the samples. After this, the Shapiro-Wilk statistical test of normality was applied at the 95% confidence level; the results show that the sample follows a normal distribution.

Given the absence of outliers, the next step was the application of Student's t-test to assess distribution trends; that is, to determine whether the sample results are within the acceptance or rejection range. For a confidence interval equal to 90% ($\alpha = 0.10$), that is, $1 - \alpha$, taking as reference the XYZ coordinates of the 20 checkpoints obtained in the field, and assuming 19 degrees of freedom, the acceptable threshold value limit of t90 (19) tabulated is 1.729. Applying Eq. (5), it was found that the tcal for all axes presented a small bias, with a tcal −6.095, −7.091, and 8.971 for the E, N, and Z axes, respectively (Table 4).

These results demonstrate a directional bias in both products, the orthomosaic and MDS, which means that there is a systematic effect on the positions of the resulting products at the points tested (Figure 9A), with a mean planimetric displacement direction of 222º (Figure 9B). In the altimetric results, the data bias is positive at all points; that is, the test points showed altitude values higher than the reference points. Similar results were found by Zhou et al. (2019) when using several scanning cameras, and by Zhou et al. (2020) when using the same camera as in this research; the data bias was attributed to the delay in registering the row/column because of the use of the rolling shutter camera. But considering that the magnitude of this bias is on millimeter scale, it does not affect the precision of the survey at all.

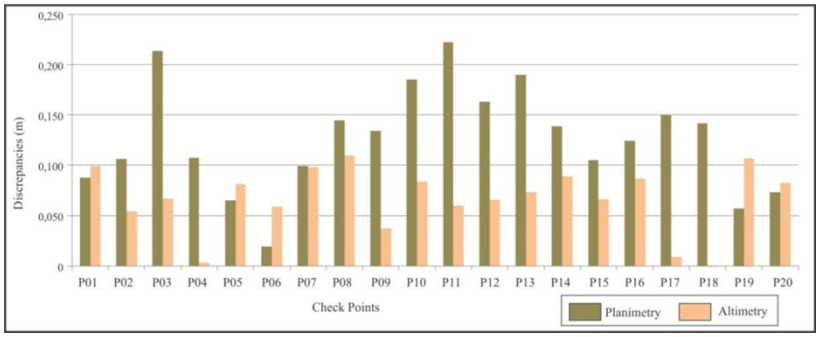

Figure 7 Positional discrepancies obtained from the orthomosaic and MDS.

Table 3 Classification of the results according to the PEC-PCD.

Planimetry	Scale	Class	PEC (m)	Average discrepancy			Condition ΔP +90% ≤ PEC	Classification
				E	N	ΔP		
	1:1,000	A	0.28	−0.081	0.093	0.126	100%	Approved
Altimetry	**Scale**	**Class**	**PEC (m)**	**Average discrepancy Z**			**Condition ΔZ +90% ≤ PEC**	**Classification**
	1:1,000	A	0.27	0.074			100%	Approved

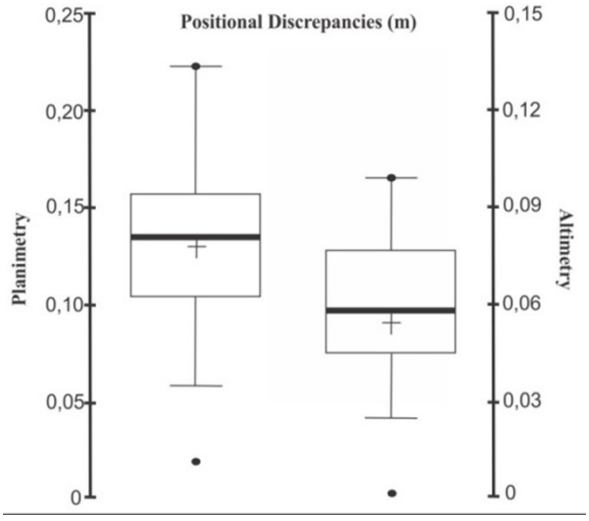

Figure 8 Boxplot with positional planimetric and altimetric discrepancies.

Table 4 Results of Student's t-test and classification.

Planimetry and altimetry	Samples	*t*90% tabulated (*t* tab)	*t* Calculated (t cal)			Condition	Classification
			E	N	Z		
	20	1,789	-6,095	-7,091	8,971	t cal ≤ t tab	Biased

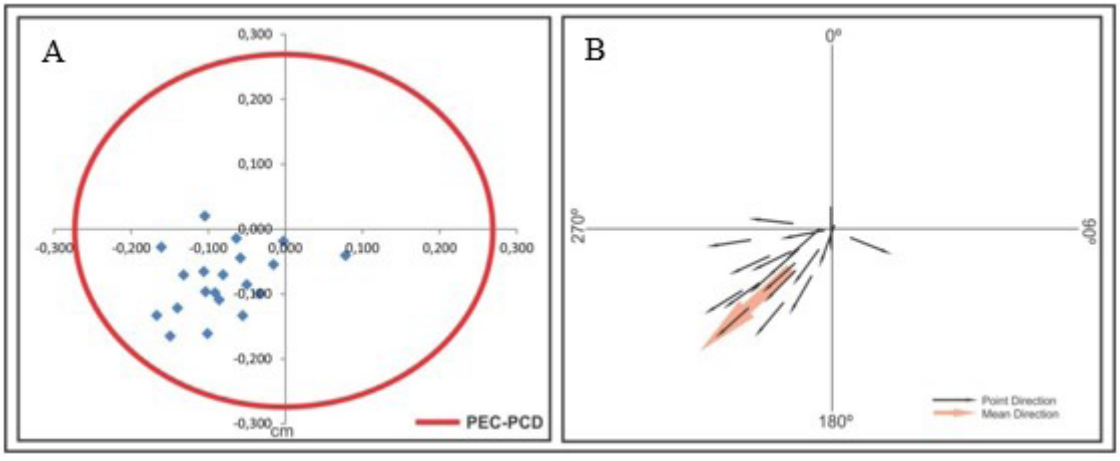

Figure 9 A. Biased planimetric distribution of the points tested; B. Direction vector of the reference positions to be tested.

To check the accuracy of the results, the chi-square test was used, following Merchant (1982), Galo and Camargo (1994), Leal (1998), Silva and Nazareno (2009), Nazareno et al. (2009), and Côrtes (2010). In all axes, the results were lower than the tabulated limit, with a chi squared of 4.566 cm, 3.314 cm, and 0.795 cm in E, N, and Z, respectively (Table 5). The results demonstrate the high precision of the survey, with values about 8 times lower than the tabulated limit in the planimetry and 33 times lower in the altimetry. The results are summarized in Table 5.

Finally, the NDE was calculated and compared with the expected EP for a given scale and class of the PEC-PCD (for planimetry) or scale (equidistance of the level curves) and class of the PEC-PCD (for altimetry). The NDE values were 0.099 m, 0.093 m, and 0.074 m in E, N, and Z, respectively (Table 6). The expected maximum planimetric and altimetric EP is 0.17 m for digital cartographic documents on the scale of 1: 1,000 in class A of the PEC-PCD. Thus, both the orthomosaic and the MDS can be classified as PEC-PCD Class A.

5 Conclusion

As explained in this paper, a number of studies have demonstrated the feasibility of using UAVs for the generation of accurate cartographic products for a given scale and class. Most of the studies use a conventional method, performing the aerial survey with a UAV and doing photogrammetric processing supported by ground control points (GCPs) materialized in the field. This paper is innovative in that we carried out an aerial survey with a UAV using a single GCP, with coordinate correction based on the PPK geodesic technique, which allows for the generation of georeferenced images with centimeter accuracy. This technique results in a faster and less expensive process, requiring less time and fewer people in the field. It also requires a smaller investment cost: there is no need to buy two expensive GNSS receivers, as there is only one stationary base receiver. The paper also presents an alternative configuration of a UAV-mounted GNSS system, comparable with the commercial RTK UAVs available on the market.

To validate the study, we ensured that there was a good distribution of checkpoints, allowing us to cross-check the coordinates of these points according the accuracy range limits described in the current technical standards. In addition, the Shapiro-Wilk statistical test revealed no outliers, attesting that the sample follows a normal distribution.

The means of the planimetric and altimetric discrepancies were significantly lower than the tabulated values in the PEC-PCD for class A on a 1:1,000 scale. The standard deviation for precision and accuracy was similar to that of UAV-based surveys using several control points. In terms of bias analysis, the products presented a small scale bias, as the test points and the MDS showed practically unidirectional planimetric displacement. Nevertheless, the results are considered adequate for the proposed scale and for the purposes of this kind of aerial survey (for mapping mines and quarries on a daily basis).

With regard to precision, the chi-square test demonstrated that the orthomosaic and the MDS have high precision, with resulting values much lower than the tabulated limits. Finally, the NDE showed lower results than the EP on both axes, demonstrating the generation of an accurate planimetric and altimetric PEC-PCD product for the 1: 1,000 scale.

Therefore, this research demonstrates the feasibility of using a UAV for the generation of orthomatics and MDS on the scale of 1:1,000 in class A of the PEC-PCD with high spatial resolution. To correct the positional bias, the simple translation technique using the average of the positions is suggested.

Table 5 Results of the chi-square test.

Planimetry and altimetry	Samples	X^2 table	X^2 calculated			Condition	Classification
			E	N	Z		
	20	27.204	4.656	3.314	0.795	$X^2 \leq X^2$ Table	Precise

Table 6 Classification of the NDE results.

Planimetry	Scale	Class	EP (m)	EQM calculated		Condition	Classification
				E	N		
	1:1,000	A	0.17	0.099	0.093	EQM ≤ EP	Approved
Altimetry	**Scale**	**Class**	**EP (m)**	**EQM calculated Z**		**Condition**	**Classification**
	1:1,000	A	0.17	0.074		EQM ≤ EP	Approved

6 References

Alves Jr., L.R., Côrtes, J.B.R., Ferreira, M.E. & Silva, J.R. 2015, 'Validação de ortomosaicos e modelos digitais de terreno utilizando fotografias obtidas com câmera digital não métrica acoplada a um VANT', *Revista Brasileira de Cartografia*, vol. 67, no. 7, pp. 1453-66.

Bolkas, D. 2019, 'Assessment of GCP Number and Separation Distance for Small UAS Surveys with and without GNSS-PPK Positioning', *Journal of Surveying Engineering,* vol. 145, no. 3, pp. 1-17, DOI:10.1061/(ASCE)SU.1943-5428.0000283.

Brasil. 1984. Decreto n. 89.817, de 20 junho de 1984. *Normas Técnicas da Cartografia Nacional*. Brasília, DF.

Bruch, A.F., Cirolini, A., Thum, A.B. & Carneiro, M. 2019, 'Avaliação da Acurácia das Cubagens de Volumes de Mineração através de Levantamentos Convencionais e Fotogramétricos', *Revista Brasileira de Geografia Física*, vol. 12, no. 1, p. 283-98, 2019, DOI:10.26848/rbgf.v12.1.p283-298.

Collischonn, C. & Matsuoka, M.T. 2016, 'Proposta de método de rede GNSS por PPP e análise de confiabilidade', *Boletim de Ciências Geodésicas*, vol. 22, no. 3, pp. 453-71. DOI:10.1590/S1982-21702016000300026.

CONCAR - Comissão Nacional de Cartografia. 2011. *Especificação Técnica para a Aquisição de Dados Geoespaciais Vetoriais*. *Infraestrutura Nacional de Dados Espaciais*, 2nd edn, Exército Brasileiro – CONCAR-EB, Brasil.

Côrtes, J.B.R. 2010, 'Análise da estabilidade geométrica de câmaras digitais de baixo custo com diferentes métodos de calibração', Tese de Doutorado, Universidade Federal do Paraná.

Elias, E.N.N., Miranda, P.C.A., Cunha, A.A. & Fernandes, V.O. 2017, 'Aplicação do Padrão de Exatidão Planimétrica para produtos cartográficos digitais (PEC-PCD)', *Simpósio Regional de Geoprocessamento e Sensoriamento Remoto*, Salvador, pp. 248-52.

Fonseca Neto, F.D., Gripp Jr., J., Botelho, M.F., Santos, A.P., Nascimento, L.A. & Fonseca, A. L.B. 2017, 'Avaliação da qualidade posicional de dados espaciais gerados por VANT utilizando feições pontuais e lineares para aplicações cadastrais', *Boletim de Ciências Geodésicas*, vol. 23, no. 1, pp. 134-49, DOI:10.1590/S1982-21702017000100009.

Fonseca Neto, F.D. 2018, 'Avaliação da Acurácia Posicional de Ortofotos Geradas por SISVANT'. Tese de Doutorado, Universidade Federal de Viçosa.

Galo, M. & Camargo, P.O. 1994, 'Utilização do GPS no controle de qualidade de cartas', *I° Congresso Brasileiro de Cadastro Técnico Multifinalitário*, Santa Catarina, pp. 41-8.

Kurkov, V.M. & Kiseleva, A.S. 2020, 'DEM Accuracy Research Based On Unmanned Aerial Survey Data', *The International Archives of the Photogrammetry, Remote Sensing and Spatial Information Sciences*, vol. XLIII-B3-2020, pp. 1347-52. DOI:10.5194/isprs-archives-XLIII-B3-2020-1347-2020.

Leal, E.M. 1998, 'Análise da qualidade posicional em bases cartográficas geradas em cad', Dissertação de Mestrado, Universidade Federal do Paraná.

Lose, L.T., Chiabrando, F. & Tonolo, F.G. 2020, 'Are Measured Ground Control Points Still Required in UAV Based Large Scale Mapping? Assessing the Positional Accuracy of an RTK Multi-Rotor Platform', *The International Archives of the Photogrammetry, Remote Sensing and Spatial Information Sciences*, vol. XLIII-B1-2020, pp. 507-14, DOI:10.5194/isprs-archives-XLIII-B1-2020-507-2020.

Menezes, R.R.V., Lisboa, M.H.M., Santos, A.P. & Dias, J.S. 2019, 'Avaliação da acurácia planimétrica das imagens do Google Earth para produção de base cartográfica', *Revista Brasileira de Cartografia*, vol. 71, no. 2, pp. 367-91, DOI:10.14393/rbcv71n2-46327.

Merchant, D.C. 1982, 'Spatial Accuracy for Large Scale Line Maps', *Proceedings of the Technical Congress of Surveying and Mapping,* pp. 222-31.

Monico, J.F.G. 2008, *Posicionamento pelo GNSS: Descrição, Fundamentos e aplicações*, 2nd edn, Editora UNESP, São Paulo.

Montgomery, D.C. & Runger, G.C. 2016, *Estatística Aplicada e Probabilidade para Engenheiros*, 6nd edn, Editora LTC, Rio de Janeiro.

Munaretto, L.A.C. 2017, *VANT e aspectos operacionais de voo*, 2nd edn, Editora DCA-BR, São José dos Campos.

Nazareno, N.R.X., Ferreira, N.C. & Macedo, F.C. 2009, 'Avaliação da Exatidão Cartográfica da Ortoimagem Quickbird e da Ortofoto Digital do Município de Goiânia', *XIV Simpósio Brasileiro de Sensoriamento Remoto*, Natal, pp. 1771-8.

Oliveira, D.V. & Brito, J.L.S. 2019, 'Avaliação da acurácia posicional de dados gerados por aeronave remotamente pilotada', *Revista Brasileira de Cartografia*, vol. 71, no. 4, pp. 934-59, DOI: https://doi.org/10.14393/rbcv71n4-50086

Ribeiro Jr., S. 2011, 'Determinação de volumes em atividades de mineração utilizando ferramentas do sensoriamento remoto', Tese de Doutorado, Universidade Federal de Viçosa.

Santos, L.F.B. 2016, 'Avaliação de modelo digital de terreno gerado através de VANT em planícies pantaneiras', Monografia, Universidade Federal do Mato Grosso, Cuiabá.

Santos, A.P., Rodrigues, D.D., Santos, N.T. & Gripp Jr., J. 2016a, 'Avaliação da acurácia posicional em dados espaciais utilizando técnicas de estatística espacial: proposta de método e exemplo utilizando a norma brasileira', *Boletim de Ciências Geodésicas*, vol. 22, no. 4, pp. 630-50, DOI:10.1590/S1982-21702016000400036.

Santos, A.P., Medeiros, N.G., Santos, G.R. & Rodrigues, D.D. 2016b, 'Avaliação da acurácia posicional planimétrica em modelos digitais de superfície com o uso de feições lineares', *Boletim de Ciências Geodésicas*, vol. 22, no. 1, pp. 157-74, DOI:10.1590/S1982-21702016000100009.

Silva, C.A. 2015, 'Avaliação da acurácia dos ortomosaicos e modelos digitais do terreno gerados por vant e sua aplicação no cálculo de volume de pilhas de rejeito da pedra cariri', Dissertação de Mestrado, Universidade Federal do Ceará, Fortaleza.

Silva, C. A., Duarte, C.R., Souto, M.V.S., Santos, A.L.S., Venerando, E.A., Bicho, C.P. & Sabadia, J.A.B. 2016, 'Avaliação da acurácia do cálculo de volume de pilhas de rejeito utilizando VANT, GNSS e LIDAR, *Boletim de Ciências Geodésicas*, vol. 22, no. 1, pp. 73-94, DOI:10.1590/S1982-21702016000100005.

Silva, L.A. & Nazareno, N.R.X. 2009, 'Análise do padrão de exatidão cartográfica da imagem do Google Earth tendo como área de estudo a imagem da cidade de Goiânia', *Simpósio Brasileiro de Sensoriamento Remoto*, Natal, pp. 1723-30.

Taddia, Y., Stecchi, F. & Pellegrinelli, A. 2020, 'Coastal Mapping Using DJI Phantom 4 RTK in Post-Processing Kinematic Mode', *Drones*, vol. 4, no. 2, pp. 1-19. DOI:10.3390/drones4020009.

Tomastík, J., Mokros, M., Surovy, P., Grznárová, A. & Merganic, J. 2019, 'UAV RTK/PPK Method-An Optimal Solution for Mapping Inaccessible Forested Areas?*', Remote Sens*, vol. 11, no. 6, e721, DOI:10.3390/rs11060721.

Yu, J.J., Kim, D.W., Lee, E.J. & Son, S.W. 2020, 'Determining the Optimal Number of Ground Control Points for Varying Study Sites through Accuracy Evaluation of Unmanned Aerial System-Based 3D Point Clouds and Digital Surface Models', *Drones*, vol. 4, no. 3, e49, DOI:10.3390/drones4030049.

Zhang, H., Aldana-Jague, E., Clapuyt, F., Wilken, F., Vanacker, V. & Van Oost, K. 2019, 'Evaluating the Potential of Post-Processing Kinematic (PPK) Georeferencing for UAV-Based Structure-from-Motion (SfM) Photogrammetry and Surface Change Detection', *Earth Surface Dynamics*, vol. 7, no. 3, pp. 807-27, DOI:10.5194/esurf-7-807-2019.

Zhou, Y., Daakir, M., Rupnik, E. & Pierrot-Deseilligny, M. 2020, 'A Two-Step Approach for the Correction of Rolling Shutter Distortion in UAV Photogrammetry', *ISPRS Journal of Photogrammetry and Remote Sensing*, vol. 160, pp. 51-66, DOI:10.1016/j.isprsjprs.2019.11.020.

Zhou, Y., Rupnik, E., Meynard, C., Thom, C. & Pierrot-Deseilligny, M. 2019, 'Simulation and analysis of photogrammetric UAV image blocks-influence of camera calibration error', *Remote Sensing*, vol. 12, no. 1, e22, DOI:10.3390/rs12010022.

Author contributions
Marciano Carneiro: conceptualization; formal analysis; methodology; writing-original draft; investigation. **Rodrigo de Lemos Peroni:** conceptualization; writing – review and editing; supervision; visualization. **Alexandre Felipe Bruch:** formal analysis; methodology validation. **Angélica Cirolini:** methodology; writing – original draft; writing – review and editing. **Adriane Brill Thum:** validation.

Conflict of interest
The authors declare no potential conflict of interest.

Data availability statement
Scripts and code are available on request.

Funding information
Not applicable.

Editor-in-chief
Dr. Claudine Dereczynski.

Associate Editor
Dr. Silvio Roberto de Oliveira Filho

How to cite:
Carneiro, M., Peroni, R.L., Bruch, A.F., Cirolini, A. & Thum, A.B. 2022, 'New Methodology for Precise UAV Surveys with a Single Ground Control Point', *Anuário do Instituto de Geociências,* 45:44874. https://doi.org/10.11137/1982-3908_45_44874